

PAPER

In-Plane Magnetization-Induced Corner States in Bismuthene

To cite this article: Bin Han *et al* 2022 *Chinese Phys. Lett.* **39** 017302

View the [article online](#) for updates and enhancements.

You may also like

- [Topological bounded corner states induced by long-range interactions in Kagome lattice](#)
Yu-Zeng Li, Zheng-Fang Liu, Xun-Wei Xu et al.
- [Entanglement in a second-order topological insulator on a square lattice](#)
Qiang Wang, Da Wang and Qiang-Hua Wang
- [Realization of hierarchical topological transitions and high-Q-response corner states in second-order topological photonic crystals](#)
Guochao Wei, Yuchen Liu, Zhenzhen Liu et al.

In-Plane Magnetization-Induced Corner States in Bismuthene

Bin Han(韩彬)^{1,2}, Junjie Zeng(曾俊杰)^{1,2}, and Zhenhua Qiao(乔振华)^{1,2*}¹ICQD, Hefei National Laboratory for Physical Sciences at Microscale,
University of Science and Technology of China, Hefei 230026, China²CAS Key Laboratory of Strongly Coupled Quantum Matter Physics, and Department of Physics,
University of Science and Technology of China, Hefei 230026, China

(Received 27 October 2021; accepted 9 December 2021; published online 29 December 2021)

We theoretically demonstrate that the electronic second-order topological insulator with robust corner states, having a buckled honeycomb lattice, can be realized in bismuthene by inducing in-plane magnetization. Based on the sp^3 Slater–Koster tight-binding model with parameters extracted from first-principles results, we show that spin-helical edge states along zigzag boundaries are gapped out by the in-plane magnetization whereas four robust in-gap electronic corner states at the intersection between two zigzag boundaries arise. By regulating the orientation of in-plane magnetization, we show different position distribution of four corner states with different energies. Nevertheless, it respects some spatial symmetries and thus can protect the higher-order topological phase. Combined with the Kane–Mele model, we discuss the influence of the magnetization orientation on the position distribution of corner states.

DOI: 10.1088/0256-307X/39/1/017302

The discovery of \mathbb{Z}_2 topological insulators (TIs)^[1–5] which exhibit spin-helical gapless edge modes protected by time-reversal symmetry, has ignited one of the most active fields in physics research. Recently, topological phases have been generalized to higher order.^[6–12] While a conventional TI in d dimensions has topological gapless states on its $(d-1)$ -dimensional boundary, a higher-order TI with n th order has topological gapless states on its $(d-n)$ -dimensional boundary. In two-dimensional (2D) higher-order TIs, pioneering theoretical works suggest the presence of 0D corner states inside the band gap of the insulating edge and bulk.^[6,7,9,13–16] Currently, 0D corner states of 2D higher-order TI have been realized in various classical photonic^[17–25] and phononic crystals.^[26–32] However, only limited 2D second-order TI material candidates have been proposed.^[9,33–40] Experimentally, electronic corner states characterizing 2D higher-order TIs have not yet been observed. Thus, it remains a big challenge to search realistic 2D electronic higher-order TI materials.

In this Letter, we theoretically propose to realize electronic higher-order TI from bismuthene, which is a 2D TI, by applying an in-plane magnetization. By introducing the in-plane magnetization, we show that the spin-helical edge modes along the zigzag boundaries become gapped, whereas four robust in-gap corner states appear at the intersect between two zigzag boundaries. The fractional charge appears at each corner with $e/2$. By applying different strengths of in-plane magnetization in bismuthene, we get differ-

ent topological phases. Without magnetization, bismuthene is a \mathbb{Z}_2 TI. By applying strong enough magnetization, it shows Chern TI phase, which is similar to the situation as reported in graphene^[41,42] and iron-halogenide.^[43] In the presence of strength between two cases, we demonstrate that there is a second-order TI phase with electronic corner states. Different orientations of magnetization will decide the position distribution of corner states, but it has no effect on the number of corner states by further analysis of the Kane–Mele model.

Model Hamiltonian. In our study, we focus on the Slater–Koster tight-binding Hamiltonian constructed by employing the two-center approximation on the orthogonal basis of $\{|A\rangle, |B\rangle\} \otimes \{|s\rangle, |p_x\rangle, |p_y\rangle, |p_z\rangle\} \otimes \{|\uparrow\rangle, |\downarrow\rangle\}$,^[44]

$$H = \sum_{i\alpha} \epsilon_\alpha c_{i\alpha}^\dagger c_{i\alpha} - \sum_{i\alpha, j\beta} t_{ij, \alpha\beta} c_{i\alpha}^\dagger c_{j\beta} + t_{SO} \sum_i c_{i\alpha}^\dagger \mathbf{l} \cdot \mathbf{s} c_{i\beta} + \lambda \sum_{i\alpha} c_{i\alpha}^\dagger \hat{\mathbf{m}} \cdot \mathbf{s} c_{i\alpha} + \Delta \sum_{z\alpha} c_{z\alpha}^\dagger c_{z\alpha}, \quad (1)$$

where $c_{i\alpha}^\dagger = (c_{i\alpha\uparrow}^\dagger, c_{i\alpha\downarrow}^\dagger)$ is the creation operator of an electron at the i th atomic site with \uparrow/\downarrow and α/β representing spin up/down and different orbitals, respectively. The first term is the on-site energy, which is degenerate for p_x and p_y orbitals due to threefold rotation symmetry. The second term stands for the hopping energy up to next-nearest neighbors with an

*Corresponding author. Email: qiao@ustc.edu.cn

© 2022 Chinese Physical Society and IOP Publishing Ltd

amplitude of $t_{ij,\alpha\beta}$. The third term represents the intra-atomic spin-orbit coupling (SOC) of strength t_{SO} with $\mathbf{s} = (s_x, s_y, s_z)$ and $\mathbf{l} = (l_x, l_y, l_z)$ being the Pauli matrices and orbital-angular-momentum operators, respectively. The fourth term corresponds to an exchange coupling between the electron and magnetization, where the unit vector $\hat{\mathbf{m}}$ denotes the direction of the exchange field. The last term is the extra potential energy on the atoms in edge of the sample, which is degenerate for orbitals and spins. This tight-binding model is generally valid for lattices with s and p orbitals. Without loss of generality, we perform our numerical study by employing the parameters of bismuthene,^[44] which are extracted from first-principles calculation by using nonlinear least-squares fitting. We calculate the Chern number by integrating the Berry curvature over the first Brillouin zone according to the formula^[41,45,46]

$$C = \frac{1}{2\pi} \sum_n \int_{\text{BZ}} d^2k \Omega_n(\mathbf{k}), \quad (2)$$

where Ω_n is the Berry curvature at momentum \mathbf{k} of the n th band. The Chern number C of the system in the presence of strong SOC, strong and weak magnetizations correspond to $C = 0$ and $C = -2$, respectively.

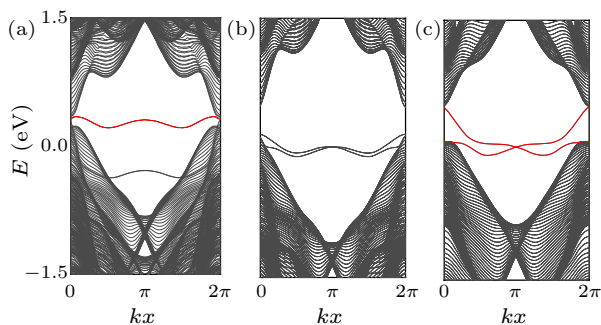


Fig. 1. Energy bands of the zigzag nanoribbon. (a) $C = 1$ TI with $t_{\text{SO}} = 0.2 \text{ eV}$ and $\lambda = 0.3 \text{ eV}$. (b) Topologically trivial band insulator with $t_{\text{SO}} = 0.2 \text{ eV}$ and $\lambda = 0 \text{ eV}$. (c) \mathbb{Z}_2 TI with $t_{\text{SO}} = 0.55 \text{ eV}$ and $\lambda = 0 \text{ eV}$. $\Delta = 0 \text{ eV}$ for all. The magnetization orientation is along the x direction. Topological edge states are highlighted in red.

We get different phases with different intra-atomic SOC strengths t_{SO} and magnetization strengths λ . We set $\Delta = 0 \text{ eV}$. As shown in Fig. 1(a), we get $C = 1$ Chern TI with $t_{\text{SO}} = 0.2 \text{ eV}$ and $\lambda = 0.3 \text{ eV}$, which has one topological edge state. As shown in Fig. 1(b), we get topologically trivial band insulator with $t_{\text{SO}} = 0.2 \text{ eV}$ and $\lambda = 0 \text{ eV}$, which has no topological edge state. As shown in Fig. 1(c), we get \mathbb{Z}_2 TI with $t_{\text{SO}} = 0.55 \text{ eV}$ and $\lambda = 0 \text{ eV}$, which has two topological edge states. As shown in phase diagram of bismuthene, bismuthene will go through a transition state from \mathbb{Z}_2 TI to Chern TI. There may be a new topological phase.

Corner States. Here, we show the emergence of corner states. Hereinbelow, we set $t_{\text{SO}} = 0.55 \text{ eV}$,

$\lambda = 0.2 \text{ eV}$ and $\Delta = 0.5 \text{ eV}$ without loss of generality, and take $\hat{\mathbf{m}}$ along the \hat{x} direction. As shown in Fig. 2(a), we first consider the corners between two zigzag-edged boundaries. In the absence of the magnetization and strong SOC, bismuthene is a 2D \mathbb{Z}_2 TI, where a pair of spin-helical gapless edge modes counterpropagate along the zigzag boundary. In the presence of magnetization, the time-reversal symmetry is broken and the edge modes become gapped as shown in Fig. 2(b) by the energy bands in red, which are two-fold degenerate. It should be noted that magnetization is not strong enough to realize Chern TI. We choose parameters that meet $C = 0$. Interestingly, when two gapped zigzag boundaries encounter each other at a corner in the diamond-shaped nanoflake, in-gap states arise as displayed in red, where the energy levels are plotted as shown in Fig. 2(c). There are four corner states, which are two pairs of degenerate energy states distributed on two different diagonals, respectively. For every corner state, the probability of wavefunctions is high-lighted in the inset, where the $1/2$ electron charge is found to localize at each corner leading to the fractionalized charge distribution. It is a key to add extra potential energy on edge atoms, which leads the gap of edge states induced by magnetization to move into the bulk energy gap. Finally, we get a global gap in energy band of zigzag nanoribbon.

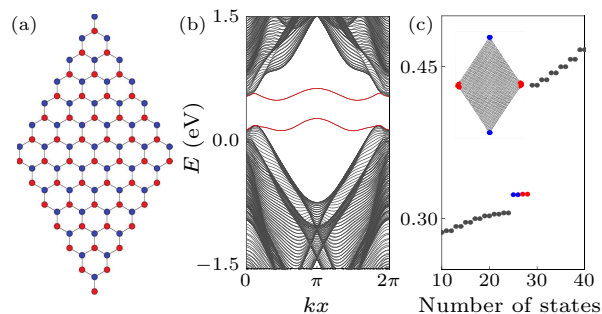


Fig. 2. Corner states in bismuthene. (a) Schematic plot of diamond-shaped buckled honeycomb lattice nanoflake with zigzag boundaries. (b) Energy bands of the zigzag nanoribbon. (c) Energy levels for diamond-shaped nanoflake. Corner states with different eigenvalues are highlighted in blue and red, respectively. Probabilities of two corner states with different eigenvalues are plotted in corresponding colors in the inset.

Results and Discussions. Now, let us analyze the physical origin of the corner states. Without magnetization, the presence of SOC leads to energy band reversal and thus drives bismuthene to \mathbb{Z}_2 TI phase. As the magnetization increases, the energy gap becomes smaller, until it is closed and reopened to lead to Chern TI phase. Although the presence of the in-plane magnetization, which is not strong enough to close the energy gap, breaks time-reversal symmetry and thus drives the \mathbb{Z}_2 TI phase into a trivial insulator, it preserves various space symmetries. For exam-

ple, in-plane magnetization breaks \mathcal{M}_z symmetry, but in-plane mirror-reflection is preserved. At this time, bismuthene is not a trivial insulator but a second-order TI with robust corner states. If magnetization is strong enough to reopen an energy gap, bismuthene will become Chern insulator phase.

Table 1. Different position distribution of corner states in different orientations of magnetization in bismuthene. Here α and β represent acute angles and obtuse angles of diamond-shape nanoflake, respectively. The position distribution is given from low to high energy of different pairs of corner states.

Orientation(ϕ)	Distribution	Orientation(ϕ)	Distribution
0	$\alpha\beta$	$\pi/2$	$\alpha\beta$
$\pi/12$	$\beta\alpha$	$7\pi/12$	$\beta\beta$
$\pi/6$	$\beta\alpha$	$2\pi/3$	$\beta\beta$
$\pi/4$	$\beta\alpha$	$3\pi/4$	$\beta\beta$
$\pi/3$	$\alpha\beta$	$5\pi/6$	$\alpha\beta$
$5\pi/12$	$\alpha\beta$	$11\pi/12$	$\alpha\beta$

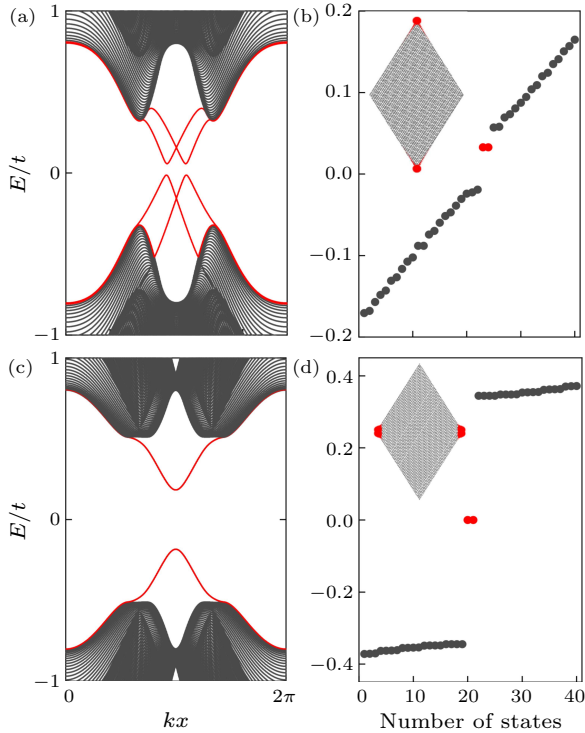


Fig. 3. Edge spectra for the modified Kane–Mele model: (a) and (b) with Rashba SOC ($\lambda_R = 0.4t$) and out-plane magnetization ($\lambda = 0.2t$), (c) and (d) with the in-plane magnetization ($\lambda = 0.2t$); (a) and (c) the energy band of zigzag nanoribbon, (b) and (d) the energy levels for diamond-shaped nanoflake. Corner states are highlighted in red. Probabilities of the corresponding corner states are plotted in the insets.

Furthermore, let us discuss the influence of the orientation of in-plane magnetization on the position distribution of the corner states. If we change the in-plane magnetization orientation sequentially by a fixed angle $\pi/12$, we can find that there is a period of $\pi/4$ about position distribution of corner states from

0 to 2π . In a period of $\pi/4$, corner states's distribution remains the same. As shown in Table 1, we get different position distribution of corner states in different orientations of magnetization. If magnetization orientations are in different periods, the position distribution of corner states will be different. We can speculate that in a 2D higher-order TI, the orientation of the magnetic field is an important or even the only factor that affects the position distribution of corner states.

We extend our findings to the other 2D TI, such as the modified Kane–Mele model. This model is defined on a honeycomb lattice, with

$$H = -t \sum_{\langle i,j \rangle} c_i^\dagger c_j + it_{\text{SO}} \sum_{\langle\langle i,j \rangle\rangle} \nu_{ij} c_i^\dagger s_z c_j + i\lambda_R \sum_{\langle i,j \rangle} c_i^\dagger (\mathbf{s} \times \mathbf{d}_{ij})_z c_j + \lambda \sum_i c_i^\dagger \mathbf{B} \cdot \mathbf{s} c_i, \quad (3)$$

where $c_i^\dagger = (c_{i\uparrow}^\dagger, c_{i\downarrow}^\dagger)$ is the creation operator of an electron at the i th atomic site with up-spin and down-spin (\uparrow/\downarrow). The first term is the nearest-neighbor hopping with an amplitude of t . The second term stands for the intrinsic SOC involving next-nearest-neighbor hopping with $\nu_{ij} = \hat{\mathbf{d}}_i \times \hat{\mathbf{d}}_j / |\hat{\mathbf{d}}_i \times \hat{\mathbf{d}}_j|$, where $\hat{\mathbf{d}}_{ij}$ is a unit vector pointing from site j to i . The third term is the nearest neighbor Rashba term, which explicitly violates the $z \rightarrow -z$ mirror symmetry. The last term is the Zeeman field along the direction of $\mathbf{B} = (\sin \theta \cos \phi, \sin \theta \sin \phi, \cos \theta)$ with a strength of λ , and θ/ϕ represent polar/azimuthal angles.

The edge states of \mathbb{Z}_2 TI in this model are both protected by time-reversal symmetry and mirror symmetry $\mathcal{M}_z = -i\sigma_z$. The presence of in-plane magnetization breaks two symmetries at the same time, but the presence of out-plane magnetization only breaks time-reversal symmetry. Extra mirror symmetry can be removed by the Rashba SOC in the third term. As shown in Fig. 3, we get two ways to realize 2D higher-order topological corner states by applying out-plane magnetization [see Figs. 3(a) and 3(b)] and in-plane magnetization [see Figs. 3(c) and 3(d)], respectively. The role of Rashba term ensures that \mathcal{M}_z symmetry is broken, which coexists with out-of-plane magnetization term. Finally, we get two different position distributions of corner states in diamond-shaped nanoflake. Interestingly, by adjusting the ratio of the in-plane and out-of-plane magnetization, the position distribution of two kinds of corners states can be transformed into each other. Different orientations of magnetization determines the position distribution of corner states. However, the number of corner states is independent of the orientation of magnetization. This has a similar effect on adjustment of the magnetic field in the above bismuthene tight-binding model. Therefore, we demonstrate that the position distribution of corner

states is indeed changed by the direction of the magnetic field in 2D higher-order TIs.

In summary, we realize electronic 2D higher-order TI by introducing in-plane magnetization. In-plane magnetization breaks time-reversal symmetry, which destroys the \mathbb{Z}_2 TI phase. In the calculation based on the Slater–Koster tight-binding model, the first order edge modes become gapped and four robust corner states are in the gap. It shows that bismuthene is a candidate to realize 2D higher-order topological insulator experimentally. Meanwhile, we find that the orientation of in-plane magnetization will affect the position distribution of corner states in bismuthene. Furthermore, we find that the orientation of magnetization will affect the position distribution of corner states in the Kane–Mele model. Therefore, the orientation of magnetization has an important role on the position distribution of corner states in 2D higher-order TIs.

Acknowledgments. This work was financially supported by the Fundamental Research Funds for the Central Universities (Grant Nos. WK3510000010 and WK2030020032), the National Natural Science Foundation of China (Grant Nos. 11974327 and 12004369), the Anhui Initiative in Quantum Information Technologies. We are grateful to AMHPC and the Supercomputing Center of USTC for providing the high-performance computing resources.

References

- [1] Kane C L and Mele E J 2005 *Phys. Rev. Lett.* **95** 146802
- [2] Bernevig B A, Hughes T L and Zhang S C 2006 *Science* **314** 1757
- [3] Hasan M Z and Kane C L 2010 *Rev. Mod. Phys.* **82** 3045
- [4] Qi X L and Zhang S C 2011 *Rev. Mod. Phys.* **83** 1057
- [5] Ren Y, Qiao Z and Niu Q 2016 *Rep. Prog. Phys.* **79** 066501
- [6] Benalcazar W A, Bernevig B A and Hughes T L 2017 *Phys. Rev. B* **96** 245115
- [7] Benalcazar W A, Bernevig B A and Hughes T L 2017 *Science* **357** 61
- [8] Song Z, Fang Z and Fang C 2017 *Phys. Rev. Lett.* **119** 246402
- [9] Ezawa M 2018 *Phys. Rev. B* **97** 155305
- [10] Schindler F, Brzezińska M, Benalcazar W A, Iraola M, Bouhon A, Tsirkin S S, Vergniory M G and Neupert T 2019 *Phys. Rev. Res.* **1** 033074
- [11] Benalcazar W A, Li T and Hughes T L 2019 *Phys. Rev. B* **99** 245151
- [12] Li T, Zhu P, Benalcazar W A and Hughes T L 2020 *Phys. Rev. B* **101** 115115
- [13] van Miert G and Ortix C 2018 *Phys. Rev. B* **98** 081110
- [14] Langbehn J, Peng Y, Trifunovic L, von Oppen F and Brouwer P W 2017 *Phys. Rev. Lett.* **119** 246401
- [15] Wieder B J and Bernevig B A 2018 arXiv:1810.02373 [cond-mat.mes-hall]
- [16] Wang Z, Wieder B J, Li J, Yan B and Bernevig B A 2019 *Phys. Rev. Lett.* **123** 186401
- [17] Zhang W, Xie X, Hao H, Dang J, Xiao S, Shi S, Ni H, Niu Z, Wang C, Jin K, Zhang X and Xu X 2020 *Light: Sci. & Appl.* **9** 109
- [18] Xie B Y, Su G X, Wang H F, Su H, Shen X P, Zhan P, Lu M H, Wang Z L and Chen Y F 2019 *Phys. Rev. Lett.* **122** 233903
- [19] Chen X D, Deng W M, Shi F L, Zhao F L, Chen M and Dong J W 2019 *Phys. Rev. Lett.* **122** 233902
- [20] Ota Y, Liu F, Katsumi R, Watanabe K, Wakabayashi K, Arakawa Y and Iwamoto S 2019 *Optica* **6** 786
- [21] Peterson C W, Benalcazar W A, Hughes T L and Bahl G 2018 *Nature* **555** 346
- [22] Mittal S, Orre V V, Zhu G, Gorlach M A, Poddubny A and Hafezi M 2019 *Nat. Photon.* **13** 692
- [23] Hassan A E, Kunst F K, Moritz A, Andler G, Bergholtz E J and Bourennane M 2019 *Nat. Photon.* **13** 697
- [24] Zangeneh-Nejad F and Fleury R 2019 *Phys. Rev. Lett.* **123** 053902
- [25] Yang Y, Jia Z, Wu Y, Xiao R C, Hang Z H, Jiang H and Xie X C 2020 *Sci. Bull.* **65** 531
- [26] Zhang X, Wang H X, Lin Z K, Tian Y, Xie B, Lu M H, Chen Y F and Jiang J H 2019 *Nat. Phys.* **15** 582
- [27] Ni X, Weiner M, Alù A and Khanikaev A B 2019 *Nat. Mater.* **18** 113
- [28] Xue H, Yang Y, Gao F, Chong Y and Zhang B 2019 *Nat. Mater.* **18** 108
- [29] Fan H, Xia B, Tong L, Zheng S and Yu D 2019 *Phys. Rev. Lett.* **122** 204301
- [30] Zhang X, Lin Z K, Wang H X, Xiong Z, Tian Y, Lu M H, Chen Y F and Jiang J H 2020 *Nat. Commun.* **11** 65
- [31] Zhang Z, Long H, Liu C, Shao C, Cheng Y, Liu X and Christensen J 2019 *Adv. Mater.* **31** 1904682
- [32] Lin Z K, Wu S Q, Wang H X and Jiang J H 2020 *Chin. Phys. Lett.* **37** 074302
- [33] Liu B, Zhao G, Liu Z and Wang Z F 2019 *Nano Lett.* **19** 6492
- [34] Park M J, Kim Y, Cho G Y and Lee S B 2019 *Phys. Rev. Lett.* **123** 216803
- [35] Sheng X L, Chen C, Liu H, Chen Z, Yu Z M, Zhao Y X 1 and Yang S A 2019 *Phys. Rev. Lett.* **123** 256402
- [36] Su Z, Kang Y, Zhang B, Zhang Z and Jiang H 2019 *Chin. Phys. B* **28** 117301
- [37] Lee E, Kim R, Ahn J and Yang B J 2020 *npj Quantum Mater.* **5** 1
- [38] Ren Y, Qiao Z and Niu Q 2020 *Phys. Rev. Lett.* **124** 166804
- [39] Chen C, Song Z, Zhao J Z, Chen Z, Yu Z M, Sheng X L and Yang S A 2020 *Phys. Rev. Lett.* **125** 056402
- [40] Wang K T, Ren Y, Xu F, Wei Y and Wang J 2021 *Sci. China Phys. Mech. Astron.* **64** 257811
- [41] Qiao Z, Yang S A, Feng W, Tse W K, Ding J, Yao Y, Wang J and Niu Q 2010 *Phys. Rev. B* **82** 161414
- [42] Tse W K, Qiao Z, Yao Y, MacDonald A H and Niu Q 2011 *Phys. Rev. B* **83** 155447
- [43] Sui Q, Zhang J, Jin S, Xia Y and Li G 2020 *Chin. Phys. Lett.* **37** 097301
- [44] Zhong P, Ren Y, Han Y, Zhang L and Qiao Z 2017 *Phys. Rev. B* **96** 241103
- [45] Thouless D J, Kohmoto M, Nightingale M P and den Nijs M 1982 *Phys. Rev. Lett.* **49** 405
- [46] Kohmoto M 1985 *Ann. Phys.* **160** 343